C. R. Acad. Sci. Paris, Ser. I 349 (2011) 353–356

Contents lists available at ScienceDirect

C. R. Acad. Sci. Paris, Ser. I

www.sciencedirect.com

Numerical Analysis

# A finite element time relaxation method

Roland Becker [a], Erik Burman [b], Peter Hansbo [c]

[a] LMAP and INRIA Bordeaux Sud-Ouest, Université de Pau, 64013 Pau cedex, France
[b] Department of Mathematics, University of Sussex, BN1 9QH Brighton, UK
[c] Department of Mathematical Sciences, Chalmers University of Technology, S-412 62 Göteborg, Sweden

ARTICLE INFO

*Article history:*
Received 22 September 2010
Accepted after revision 4 December 2010
Available online 18 February 2011

Presented by the Editorial Board

ABSTRACT

We discuss a finite element time-relaxation method for high Reynolds number flows. The method uses local projections on polynomials defined on macroelements of each pair of two elements sharing a face. We prove that this method shares the optimal stability and convergence properties of the continuous interior penalty (CIP) method. We give the formulation both for the scalar convection–diffusion equation and the time-dependent incompressible Euler equations and the associated convergence results. This note finishes with some numerical illustrations.



RÉSUMÉ

Nous présentons une méthode d'éléments finis de type relaxation de temps pour les écoulements de fluides à grand nombre de Reynolds. Cette approche utilise des projections locales sur un espace de polynômes défini sur des macor-éléments pour chaque paire d'éléments adjacents à une face intérieure du maillage. Nous démontrons la stabilité et la convergence. Nous donnons des résultats pour l'équation de convection–diffusion et les équations instationnaires d'Euler. Cette note se termine par des résultats numériques.



## 1. Introduction

The computation of high Reynolds number flows is one of the most challenging problems in scientific computing. Indeed the nonlinear coupling of the Navier–Stokes' equations leads to small scale features in the solution even for problems with smooth data. The standard Galerkin methods, being energy conservative, will represent all the energy carrying features on the resolved scales, leading to spurious oscillations. One way to deal with this problem is to apply a filter to the continuous equation and then model the so-called Reynolds stresses, typically by a nonlinear viscosity, such as the Smagorinsky model [11]. A different more recent approach is the time-relaxation method, where a penalty term is added for the distance from the filtered to the unfiltered solution [1].

Another advocated approach is the use of stabilized finite element methods to replace the turbulence model. These methods are designed so as to have optimal convergence for smooth solutions [9,8,2,4], and to contain perturbations in an $O(h)$ region from layers. This approach is appealing for large eddy simulation since it indicates the possibility of (i) optimal convergence for smooth solutions [4]; (ii) containment of pollution caused by high frequency content due to the nonlinear coupling [5]; (iii) optimal dissipation rates in the turbulent zone [3,10]. Similar quasi-optimal convergence proofs were obtained recently for a finite element realization of the time-relaxation method [7] in the simple case of a linear transport equation.

*E-mail addresses:* roland.becker@univ-pau.fr (R. Becker), E.N.Burman@sussex.ac.uk (E. Burman), peter.hansbo@chalmers.se (P. Hansbo).

1631-073X/$ – see front matter 
doi:10.1016/j.crma.2010.12.010

Here we draw upon similarities of the symmetric stabilization and time-relaxation to propose a simplified time-relaxation method. Instead of using a global $H^1$ projection for the construction of the filtered approximation we use a local $L^2$-projection, onto a local space of smoother functions. For each face $F$ this local space is defined on the elements sharing a face.

Let $\Omega \subset \mathbb{R}^d$ be a polygonal domain with boundary $\partial\Omega$ and exterior normal $n$, $d = 2, 3$. Our model problems read

$$-\epsilon \Delta u + \beta \cdot \nabla u + u = f \in L^2(\Omega) \quad \text{in } \Omega,\ u = 0 \text{ on } \partial\Omega, \quad \text{and} \tag{1}$$

$$\partial_t u + (u \cdot \nabla) u + \nabla p = f \in \left[L^2(\Omega)\right]^2, \quad \nabla \cdot u = 0 \text{ in } \Omega,\ u \cdot n = 0 \text{ on } \partial\Omega,\ u(0) = u_0. \tag{2}$$

In problem (1) we take $\epsilon \in \mathbb{R}^+$ and $\beta \in [W^{1,\infty}(\Omega)]^2$ and $f \in L^2(\Omega)$ is the source term.

## 2. Finite element framework

Let $\{\mathcal{T}_h\}_h$, with $\mathcal{T}_h = \{K\}$, be a quasi-uniform family of meshes with $h = \max_{K \in \mathcal{T}_h} \operatorname{diam}(K)$. We denote the set of interior faces by $\mathcal{F}_h$. For each face $F \in \mathcal{F}_h$ we introduce the macro element $\hat{K}_F$ consisting of $K$ and $K' \in \mathcal{T}_h$ such that $F = K \cap K'$. We introduce the standard finite element space $V_h$ of piecewise isoparametric polynomial functions $v_h$, such that the reference polynomial space contains the set of polynomials of maximal total degree $k$, $P_k$. Moreover we introduce the local polynomial spaces associated to each face $F$

$$W_l(\hat{K}_F) := \left\{ w \in P_l(\hat{K}_F) \right\}, \quad l \geqslant 0.$$

We define the scalar products $(f, g)_\Omega := \int_\Omega f g \, \mathrm{d}x$ and $\langle f, g \rangle_{\partial\Omega} := \int_{\partial\Omega} f g \, \mathrm{d}s$ for $L^2$-functions $f$, $g$.

### 2.1. Time-relaxation and equivalence with interior penalty methods

Consider the abstract problem, find $u \in V$ such that $a(u, v) = (f, v)$ for all $v \in V$ with Galerkin approximation find $u_h \in V_h$ such that $a(u_h, v_h) = (f, v_h)$ for all $v_h \in V_h$. The idea of the time-relaxation method (see for instance [7] and references therein) is then to add a term $s(u, v)$ of the form

$$s(u, v) = \left(\tau^{-1}(u - Gu), v - Gv\right)_\Omega,$$

where $G$ is some filtering operator $G : V \mapsto W$ where $W$ is a space with functions of higher regularity. The relaxation time $\tau$ sets the dissipation rate for the scales that are filtered out by $G$, typically corresponding to the eddy turnover time. The bilinear form $s$ is symmetric and positive semi-definite.

The spurious oscillations that appears in Galerkin methods are due to energy accumulation on the highest frequencies. In the case of finite element methods the piecewise polynomial carries the approximation properties of the space, and the highest frequencies are represented by the singularities over element faces, i.e. jumps in the solution or its derivatives over element faces. It is this scale separation that naturally occurs in finite element methods that we wish to exploit here. Indeed for each interior face $F$ we let the projection $G_F$ be defined by $G_F u_h \in W_l(\hat{K}_F)$ such that

$$(G_F u_h, v_h)_{\hat{K}_F} = (u_h, v_h)_{\hat{K}_F}, \quad \forall v_h \in W_l(\hat{K}_F).$$

Clearly by the orthogonality of the projection this operator is symmetric, i.e.

$$(u_h - G_F u_h, v_h)_{\hat{K}_F} = (u_h - G_F u_h, v_h - G_F v_h)_{\hat{K}_F}. \tag{3}$$

The time-relaxation term that we propose will act on the singular part of the finite element solution only and is defined by

$$s_l(u_h, v_h) := \sum_{F \in \mathcal{F}_h} \tau_F^{-1} \left((u_h - G_F u_h), v_h\right)_{\hat{K}_F},$$

where $l$ refers to the polynomial order of the projection space $W_l(\hat{K}_F)$. Let $\tau_F := h_F / \sigma_F$ where $\sigma_F > 0$ denotes a characteristic flow velocity, that may be chosen locally provided it remains bounded away from zero. It clearly has the physical dimension of time and corresponds to the time needed to cross $K_F$. The form (3) acts on the jump of $u_h$ and all its derivatives and is therefore a generalization of the CIP method [6]. We now prove the equivalence with the multipenalty stabilization operator

$$j(u_h, v_h) := \sum_{F \in \mathcal{F}_h} \sum_{i=1}^{k} \tau_F^{-1} h_K^{2i+1} \int_F \left[D^i u_h\right]\left[D^i v_h\right] \mathrm{d}s,$$

where $[x]$ denotes the jump of quantity $x$ over the face $F$. The sign is irrelevant.

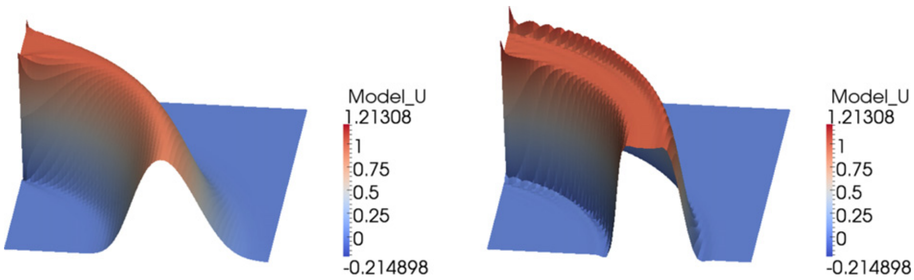


**Fig. 1.** Convection–diffusion: solution with $l = 1$ (left) and $l = 2$ (right) with 4096 elements.

**Lemma 2.1.** *Let $u_h \in W_h$ and $l \geqslant k$. Then there exists $c_1, c_2 > 0$ independent of the local mesh size, but not the local mesh geometry such that $c_1 j(u_h, u_h) \leqslant s_l(u_h, u_h) \leqslant c_2 j(u_h, u_h)$.*

**Proof.** Consider an arbitrary face $F$ with macro $\hat{K}_F$. Map them to the reference elements $\mathcal{F}$ and $\hat{\mathcal{K}}_F$ and denote the mapped functions $\widetilde{G_F u_h}$ and $\tilde{u}_h$. By norm equivalence there exists $\tilde{c}_1, \tilde{c}_2 > 0$ such that

$$\tilde{c}_1 \sum_{i=1}^{k} \int_{\mathcal{F}} \left[D^i \tilde{u}_h\right]^2 \mathrm{d}s \leqslant \int_{\hat{\mathcal{K}}_{\mathcal{F}}} (\tilde{u}_h - \widetilde{G_F u_h})^2 \,\mathrm{d}x \leqslant \tilde{c}_2 \sum_{i=1}^{k} \int_{F} \left[D^i \tilde{u}_h\right]^2 \mathrm{d}s.$$

The first inequality follows from $[D^i \widetilde{G_F u_h}] = 0$ on $\mathcal{F}$ and an inverse inequalities. For the second notice that both the time relaxation and the multipenalty induce seminorms with the same kernel consisting of the space $W_l(\hat{\mathcal{K}}_F)$. We conclude by scaling back to the physical element and summing over $F \in \mathcal{F}_h$. $\square$

**Remark 1.** Slight variations of the time-relaxation term are possible. For instance the following streamline diffusion form minimizes crosswind diffusion: $s_l(u_h, v_h) := \sum_{F \in \mathcal{F}_h} (\tau \beta \cdot \nabla(u_h - G_F u_h), \beta \cdot \nabla(v_h - G_F v_h))_{\hat{K}_F}$. Alternatively the $H^1$-projection may be used so that $(\nabla G_F u_h, \nabla v_h)_{\hat{K}_F} = (\nabla u_h, \nabla v_h)_{\hat{K}_F}$ for all $v_h \in W_l(\hat{K}_F)$. Then a variant is $s_l(u_h, v_h) := \sum_{F \in \mathcal{F}_h} (\tau \|\beta\|_{\hat{K}_F} \nabla(u_h - \alpha(u_h) G_F u_h), \nabla v_h)_{\hat{K}_F}$, where $0 \leqslant \alpha(u_h) \leqslant 1$ is a function allowing the method to degenerate to first order viscosity close to shocks.

## 3. Numerical examples

### *3.1. The convection–diffusion equation*

Let the bilinear form $a(\cdot,\cdot)$ be defined by $a(u, v) := (\beta \cdot \nabla u + u, v)_\Omega + (\epsilon \nabla u, \nabla v)_\Omega$ and the corresponding time-relaxation finite element method reads, find $u_h \in V_h^0 := V_h \cap H_0^1(\Omega)$ such that

$$a(u_h, v_h) + s_l(u_h, v_h) = (f, v_h)_\Omega, \quad \forall v_h \in V_h^0. \tag{4}$$

Consider the triple norm $|||u_h|||^2 := \|h^{\frac{1}{2}} |\beta|^{-1/2} \beta \cdot \nabla u_h\|^2_{L^2(\Omega)} + \|u_h\|^2_{L^2(\Omega)} + \|\epsilon^{\frac{1}{2}} \nabla u_h\|^2_{L^2(\Omega)}$. The following stability and convergence estimates can be proven thanks to Lemma 2.1 and the CIP-analysis [6].

**Proposition 3.1.** *Let $u_h$ be the solution of (4). Then there holds $|||u_h||| \leqslant C\|f\|^2_{L^2(\Omega)}$. Let $u$ be a sufficiently smooth solution of (1) and $u_h \in V_h^0$ the solution of (4), with $l \geqslant k$. Then*

$$|||u - u_h||| \leqslant C\big(h + |\beta|^{\frac{1}{2}} h^{\frac{1}{2}} + \epsilon^{\frac{1}{2}}\big) h^k |u|_{H^{k+1}(\Omega)}.$$

As a numerical example, we use $\Omega = ]-1, 1[^2$, $\beta = (1 + y, -(1 + x))$, $\varepsilon = 10^{-6}$ and a characteristic function on the inflow $\{-1\} \times ]-1, 1[$. All computations are done with continuous bilinear finite elements on quadrilateral meshes. The results for $l = 1$ and $l = 2$ are shown in Fig. 1.

### *3.2. The incompressible Euler's equation*

We introduce an additional time-relaxation term to stabilize the pressure velocity coupling letting $s_l(p_h, q_h) = \sum_{F \in \mathcal{F}_h} h_F^{-1} \sigma_F^{-1} ((p_h - G_F p_h), q_h - G_F q_h)_{\hat{K}_F}$. This is leads to a pressure stabilization that may be analyzed using the methods presented in [3]. The space semi-discretized time-relaxation finite element method then reads find $(u_h(t), p_h(t)) \in X_h := [V_h]^2 \times V_h$ such that

$$(\partial_t u_h, v_h)_\Omega + c(u_h; u_h, v_h) + b(p_h, v_h) - b(q_h, u_h) + s_l(u_h, v_h) + s_l(p_h, q_h) = (f, v_h)_\Omega \quad \forall v_h \in X_h, \tag{5}$$

| $N$ | $\|u-u_h\|_{L_1}$ | $\|u-u_h\|_{W_1^1}$ |
|---|---|---|
| 64 | $5.132\times10^{-2}$ | $1.129\times10^{0}$ |
| 256 | $1.304\times10^{-2}$ | $6.073\times10^{-1}$ |
| 1024 | $3.434\times10^{-3}$ | $3.281\times10^{-1}$ |
| 4096 | $9.255\times10^{-4}$ | $1.762\times10^{-1}$ |
| 16384 | $2.308\times10^{-4}$ | $8.851\times10^{-2}$ |

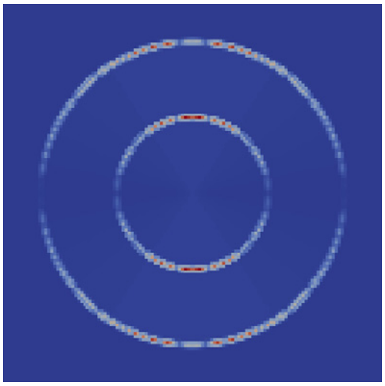

**Fig. 2.** Errors for the standing vortex problem at $t=3$ and plot of the point-wise error for the standing vortex problem.

where, with $u_{h,n}^{-} := \frac{1}{2}(u_h\cdot n - |u_h\cdot n|)$,

$$c(u_h;u_h,v_h) := \left((u_h\cdot\nabla)u_h + \frac{1}{2}(\nabla\cdot u_h)u_h, v_h\right)_{\Omega} - \langle u_{h,n}^{-}u_h, v_h\rangle_{\partial\Omega}, \quad b(p_h,v_h) := (p_h,\nabla\cdot v_h) - \langle p_h, v_h\cdot n\rangle_{\partial\Omega}.$$

Let $\|(u_h,p_h)\||_h := (\|\sqrt{|u_h\cdot n|}u_h\|^2_{L^2(\partial\Omega)} + s(u_h,u_h) + s_p(p_h,p_h))^{1/2}$. For smooth solutions to (2) the time-relaxation finite element discretization satisfies the following quasi-optimal convergence results.

**Proposition 3.2.** *Let $(u,p)$ be a sufficiently smooth solution of (2) and $(u_h,p_h)$ the solution of (5), with $l\geqslant k$. Then, with $C(u,T)\sim\exp(\|\nabla u\|_{L^\infty(\Omega)}T)$,*

$$\left\|(u-u_h)(T)\right\|^2_{L^2(\Omega)} + \int_0^T \left|\!\left|\!\left|(u_h,p_h)\right|\!\right|\!\right|_h^2 \mathrm{d}t \leqslant C(u,T)h^{2k+1}\left(|u|^2_{H^{k+1}(\Omega)} + |p|^2_{H^{k+1}(\Omega)}\right).$$

The proof of this result follows from the norm equivalence Lemma 2.1 and the analysis of [4].

As a numerical example, we consider the standing (stationary) vortex problem in the domain $\Omega = ]-1,1[^2$. The solution is given in cylindrical coordinates by $u_\theta = 0$ and $u_r = 0$ for $r\leqslant 0.4$ and $r\geqslant 0.8$, $u_\theta = 2.5r$ for $0.4\leqslant r\leqslant 0.8$, and $u_\theta = 2-2.5r$ for $r\geqslant 0.8$. We solve the discrete equations up to $t=3$ and then compute the errors in the $L_1$ and $W_1^1$ norms (the solution regularity does not allow for optimal convergence in $L^2$). The computed errors as well as a typical plot of it are shown in Fig. 2.

## References


[1] N.A. Adams, S. Stolz, A subgrid-scale deconvolution approach for shock capturing, J. Comput. Phys. 178 (2002) 391–426.

[2] R. Becker, M. Braack, A two-level stabilization scheme for the Navier–Stokes equations, in: Numerical Mathematics and Advanced Applications, Springer, Berlin, 2004, pp. 123–130.

[3] E. Burman, Interior penalty variational multiscale method for the incompressible Navier–Stokes equation: Monitoring artificial dissipation, Comput. Methods Appl. Mech. Engrg. 196 (2007) 4045–4058.

[4] E. Burman, M.A. Fernández, Continuous interior penalty finite element method for the time-dependent Navier–Stokes equations: Space discretization and convergence, Numer. Math. 107 (2007) 39–77.

[5] E. Burman, J. Guzmàn, D. Leykekhman, Weighted error estimates of the continuous interior penalty method for singularly perturbed problems, IMA J. Numer. Anal. 29 (2009) 284–314.

[6] E. Burman, P. Hansbo, Edge stabilization for Galerkin approximations of convection–diffusion–reaction problems, Comput. Methods Appl. Mech. Engrg. 193 (2004) 1437–1453.

[7] J. Connors, W. Layton, On the accuracy of the finite element method plus time relaxation, Math. Comp. 79 (2010) 619–648.

[8] J.-L. Guermond, Stabilization of Galerkin approximations of transport equations by subgrid modeling, Modél. Math. Anal. Numér. 33 (1999) 1293–1316.

[9] P. Hansbo, A. Szepessy, A velocity–pressure streamline diffusion finite element method for the incompressible Navier–Stokes equations, Comput. Methods Appl. Mech. Engrg. 84 (1990) 175–192.

[10] J. Principe, R. Codina, F. Henke, The dissipative structure of variational multiscale methods for incompressible flows, Comput. Methods Appl. Mech. Engrg. 199 (2010) 791–801.

[11] J. Smagorinsky, Some historical remarks on the use of nonlinear viscosities, in: Large Eddy Simulation of Complex Engineering and Geophysical Flows, Cambridge Univ. Press, New York, 1993, pp. 3–36.